RMetS

Royal Meteorological Society

Climatic precursors of autumn streamflow in the northeast United States

Gavin Gong,* Lucien Wang and Upmanu Lall
Department of Earth and Environmental Engineering, Columbia University, New York, NY, USA

ABSTRACT: In this study, statistical linkages between autumn streamflow in the northeast United States and preceding summer sea surface temperatures are developed to establish predictive potential for climate-informed seasonal streamflow forecasts in this region. Predictor regions with physically plausible teleconnections to local streamflow are identified and evaluated in a multivariate and nonlinear framework using local regression techniques. Three such regions are identified, located in the Bering Sea, the tropical Pacific just west of Mexico, and the tropical Atlantic off the coast of Africa. Asymmetries in each region's univariate local regression result are apparent, and bivariate local regressions are used to attribute these asymmetries to interactions with physical mechanisms associated with the other two regions, and possibly other unaccounted for climatic predictors. A bivariate model including the tropical Pacific and tropical Atlantic regions yields the strongest local regression result, explaining 0.68 of the interannual streamflow variability. An analogous multivariate linear regression analysis is only able to explain 0.20 of the streamflow variability and thus the use of nonlinear methods' results in a marked improvement in streamflow simulation capability. Cross-validation considerably weakens the streamflow forecasts using this model; however, forecast skill may improve with a longer period of record or the inclusion of additional predictors. Copyright © 2010 Royal Meteorological Society

1. Introduction

Climate-informed seasonal streamflow forecasts are increasingly recognized as a potentially viable information source for reservoir operation and water allocation. In developed regions where there is competing demand for water, climate-based forecasts offer an objective means of optimizing water allocation among stakeholders under different stress conditions. For example, forecasts of upcoming low-flow conditions will justify a reduction in reservoir releases to protect against drought, whereas forecasts of upcoming high-flow conditions will allow for an increase in reservoir releases for ecological conservation and recreation. Such forecasts can provide equitable benefits and justify sacrifices for all stakeholders.

Climate-based forecasts can be developed using either dynamical or statistical methods. Dynamical streamflow forecasts typically use observations of current climatic conditions, as input for large-scale general circulation model (GCM) simulations of atmospheric processes months into the future. The model output of future precipitation or runoff is then downscaled from GCM gridcell scales to river basin scales, and translated to streamflow via additional rainfall–runoff–streamflow conversions. In contrast, statistical streamflow forecasts typically use

observations of current climate as direct predictors of future streamflow, based on historical lead–lag statistical relationships between climate predictor and streamflow values. Dynamical linkages are not used at any point, and the historical relationship observed at seasonal timescales is presumed to hold in the future as well.

Regardless of the specific method applied, effective seasonal streamflow forecasts must have a strong physical foundation for the translation of current climate information into future streamflow magnitudes. For dynamical methods, this means reliable GCM simulations, downscaling techniques and rainfall–runoff–streamflow conversions for the specific region under consideration. For statistical methods, this means strong, robust, and physically justifiable statistical relationships between remote climate predictors and local streamflow predictands. The objective of this study is to establish such a physical foundation for the northeast United States (US), in order to demonstrate the potential for climate-informed seasonal streamflow forecasts in this region.

2. Background

2.1. Study region

The specific study region within the northeast US is the upper portion of the Delaware River Basin (DRB), located in the Catskill region of New York State, near

* Correspondence to: Gavin Gong, Department of Earth and Environmental Engineering, Columbia University, 918 Mud Hall, 500 West 120 Street, MC4711, New York, NY 10027, USA.
E-mail: gg2138@columbia.edu

Figure 1. The Delaware River Basin, with the upper basin streamflow study region boxed. (Source: http://commons.wikimedia.org/wiki/
File : Delawarerivermap.png). This figure is available in colour online at www.interscience.wiley.com/ijoc

the northeast corner of Pennsylvania (Figure 1). Three water supply reservoirs in the upper DRB provide roughly 50% of the total drinking water for New York City. A renowned trout fishery is located immediately downstream of the reservoirs, and residents along the river further downstream are susceptible to periodic flooding. Hence, there are multiple competing interests among DRB stakeholders, which pose a considerable water management challenge that can potentially be assuaged with effective climate-based seasonal streamflow forecasts.

GCMs are not known to be especially skillful in the northeast US for hydroclimatic fluxes such as precipitation, due in part to low signal to noise ratios in this region (Dirmeyer *et al.*, 2003; Marengo *et al.*, 2003; Quan *et al.*, 2006). Modest GCM skill in turn compromises the reliability of subsequent downscaling and streamflow conversions, which also have their own inherent uncertainties. Therefore, in this study, we pursue direct statistical linkages between upper DRB streamflow and preceding climatic states, based on the belief that statistical methods hold the greatest promise for seasonal streamflow forecasts in this region.

2.2. Hydroclimatological drivers

Precipitation in the upper DRB region is attributed mainly to frontal systems and cyclogenesis (Zishka and Smith, 1980; Gurka *et al.*, 1995; Hartley and Keables, 1998; Bradbury *et al.*, 2003; Vermette, 2007). A common pattern of cyclogenesis giving rise to storms in the northeast

US originates over the Gulf of Mexico or the Atlantic coast of the southeastern US and travels northeast through the Middle-Atlantic states and New England. Another common cyclogenesis pattern originates near the Great Lakes region and travels eastward, with moisture supplied from the extra-tropical Pacific, Gulf of Mexico or Atlantic Ocean. These storm tracks are supported by both the mid-latitude and sub-topical jet streams. Occasionally, tropical cyclones originating in the tropical North Atlantic track through the US northeast during the late summer and early fall. These storms often lose their tropical characteristics and bear more resemblance to mid-latitude cyclones upon reaching mid-latitudes (Vermette, 2007), but they nevertheless tend to deposit relatively large amounts of precipitation over the region. These precipitation-bearing phenomena should naturally result in elevated streamflow values for the upper DRB region.

A number of studies have searched for statistically significant and physically meaningful drivers of seasonal hydroclimate within this general region (Barlow *et al.*, 2000; Bradbury *et al.*, 2002; Joyce, 2002; Bradbury *et al.*, 2003; Jutla *et al.*, 2006; Kingston *et al.*, 2006; Sveinsson *et al.*, 2008a, 2008b). Variables such as cyclone activity, precipitation, and streamflow have been associated with climatic modes such as the El Nino-Southern Oscillation (ENSO), the North Atlantic Oscillation (NAO), the Pacific Decadal Oscillation (PDO), and the Pacific/North American Pattern (PNA), mainly during winter and spring. Hydroclimatic associations have also been made

with alternative climate descriptors such as synoptic weather patterns (Miller *et al.*, 2006) and snow depth (Gong *et al.*, 2010). However, the statistical significance is generally modest, and a consistent and coherent explanation for streamflow variability in the northeast US has yet to emerge from this body of literature. Furthermore, these relationships tend to decrease in strength and statistical significance as one moves inland from coastal New England towards the interior Middle-Atlantic region.

One likely reason for this ambiguity is that the northeast US is not geographically proximal to the major climate modes. For example, ENSO, PDO, and PNA all originate in the Pacific sector, whereas the NAO originates downgradient from the region. Northeast US hydroclimate may very well be influenced by these phenomena, but may not be strongly tied to the geographic centres of action embodied by their indices (Leathers *et al.*, 2008). An associated reason is that atmospheric moisture is supplied to this region from multiple sources, spanning from the extra-tropical Pacific to the tropical Atlantic. Thus multiple climatic drivers are likely involved, which mitigates the statistical significance of any single driver when evaluated in isolation.

Another reason is that the existing literature for this region focuses on linear regression-type relationships, whereas the climatic drivers may very well be nonlinearly related to regional hydroclimate as can be expected from the constitutive equations of ocean–atmosphere dynamics. Nonlinear methods have been utilized to develop similar hydroclimatic relationships in other regions. For example, mutual information (Fraser and Swinney, 1986; Moon *et al.*, 1995; Khan *et al.*, 2006) and related methods have been used to identify the strength of nonlinear dependence and also to select predictors (Sharma, 2000a, 2000b; Sharma *et al.*, 2000). Here, we introduce a direct approach for identifying nonlinear or linear dependence using a method that seeks to identify univariate relationships between predictors and predictands and the associated strength of relationship without a prior assumption as to the form of the nonlinearity. Continuity and differentiability of an underlying regression relationship is assumed, and an approximation to an arbitrary regression function in the spirit of Taylor series approximation under non-equal spacing of predictor values is used to form the regression function. The utility of the approach is that generalized cross-validation (GCV) is used to directly assess the potential predictability and to offer a standardized comparison of predictability across each of the individual potential predictors. Thus, although a predictive framework is used, we use it primarily in a diagnostic context to identify potential, spatially coherent regions in a climate field that contribute to the prediction of the target hydrologic variable. We do not address the problem of the selection of the best subset of predictors in this article or of the development of the associated prediction model and its testing. Rather, the focus is on the application of the method to identify potential predictors and

to discuss their physical relevance, uni- and in bivariate interactions.

2.3. Study objectives

With respect to the specific goals of this study, the existing literature on hydroclimatic teleconnections for this region has yet to establish a clear potential for climate-informed seasonal streamflow forecasts. Many of the aforementioned studies focus on climatic drivers of precipitation or storm events and infer a consequent association with streamflow, but do not explicitly identify a streamflow relationship through either landsurface hydrologic modelling or direct statistical analysis. The literature also by and large reports concurrent seasonal relationships, whereas seasonal lead–lag relationships are required to demonstrate predictive potential. Note that preceding surface temperatures and local snow cover are the two main drivers that contain seasonal memory and so can exhibit lead–lag relationships. Atmospheric drivers do not contain seasonal memory and therefore are expected to exhibit only concurrent relationships, or serve as a proxy for other drivers that contain memory.

One recent exception is Miller *et al.* (2006), which directly related spring season streamflow in a river basin adjacent to the upper DRB to synoptic weather pattern categories during the preceding winter. They found that the frequency and type of regional weather patterns to be a better indicator of subsequent streamflow than large-scale climate indices. However, these synoptic weather pattern predictors may simply be an atmospheric proxy for the actual memory-containing precursors. The anomalous water fluxes generated by these winter weather patterns are stored at the surface in the form of snow or ice that melts in the following spring and is released to streamflow. Furthermore, the weather patterns themselves are in all likelihood depositing moisture derived from oceanic sources and initiated by oceanic anomalies. Nevertheless, a linear model explaining 54% of the streamflow variance was achieved, but only after removing extreme values from the streamflow time series.

This study will establish a more robust physical foundation for seasonal streamflow forecasts in the northeast US, by addressing a number of key limitations in the existing literature. First, multiple predictor regions will be considered, as atmospheric moisture arrives in the upper DRB from a variety of sources. Initial assessments of individual regions will be complemented by groups of predictor regions in a multivariate framework. Second, sea surface temperatures (SSTs) will be investigated as the predictor variable, as the moisture sources are ultimately of oceanic origin. Use of hemispheric-scale SST fields allows for a more flexible identification of predictor regions than climate modes whose geographic centres of action are fixed. Third, nonlinear regression techniques will be utilized, as the climatic drivers of upper DRB streamflow are not necessarily linear. The ambiguous relationships reported in the literature may be a result of nonlinear behaviour being only partially captured by

linear analyses, e.g. removing extreme values in Miller *et al.* (2006) which are likely to behave nonlinearly.

3. Data and methods

Climatic precursors will be pursued for streamflow entering the Pepacton Reservoir, along the east branch of the upper Delaware River. Historical unobstructed streamflow data are obtained from US Geological Survey gauging station 01 413 500 at Margaretville, NY, located just upstream of the Pepacton Reservoir. Monthly averaged streamflow at USGS stations entering all three New York City water supply reservoirs are highly correlated, but the Pepacton Reservoir inflow has the longest continuous record spanning 68 years (1938–2006). Therefore, this record is used to represent naturally occurring streamflow variability in the upper DRB region. Historical SST data over this period is obtained from the Kaplan SST V2 dataset provided by the NOAA/OAR/ESRL PSD, Boulder, CO, USA (Kaplan *et al.*, 1998). Monthly averaged SST values are available on a $5° \times 5°$ resolution global grid, from 1856 to present.

The autumn season is selected for streamflow prediction, as this is the historical low storage season for the upper DRB reservoirs, and is also characterized by high interannual streamflow variability. Operational rule curves for the reservoirs specify the lowest storage requirements during October and November, so effective seasonal forecasts of streamflow during this 2-month period would be especially helpful to regional water managers. Therefore, average streamflow for October–November (ON) is related to average SST anomalies for the preceding August–September (AS), over the 68-year period of record. Note that snowmelt is not a contributor to autumn streamflow in this region, which leaves SSTs as the only climate driver with seasonal memory.

Nonlinear relationships are investigated using a technique known as local regression, or LOESS smoothing (Loader, 1999; Lall *et al.*, 2006; Moon *et al.*, 2008). In this method, a series of simple least-squares regression models are fit using localized subsets of the overall dataset. Each predictand is estimated using a unique subset of temporally proximal predictor values, rather than the entire set of predictors. The results of each subset model taken together comprise the final local regression relationship. A key advantage of this technique is that the final regression model is not constrained to be a single polynomial function that is applied to all data points, hence there is greater flexibility in fitting the model to the observed data. It can be used to develop multivariate as well as univariate models.

Local regression can be computationally intensive since a separate subset regression model is developed for each data point. However, the basic rationale is that nearby data points should be strongly and simply related, so that only low-degree polynomials should be required for each subset. In addition, a weighting function is usually applied so that the subset data points closer to the point being modelled factor more strongly into the local regression. Finally, the strength of the overall regression can vary with the subset size selected. Use of a very large subset approaches a standard least-squares polynomial regression, whereas a very small subset retains the random errors in the data. The subset size that yields the strongest relationship is retained as the local regression result.

For this study, the strength of the overall regression is measured using a GCV score, where a smaller GCV score indicates a stronger relationship. The subset size is expressed as an α index, where a larger α index represents a smaller subset. Also, a linear regression is fit for each localized subset, so that the local regression result for a large subset converges toward a simple linear regression model for the entire dataset. In this way, the local regression analysis does not necessarily imply a nonlinear relationship. If using the entire dataset for each local regression relationship results in the lowest GCV score, then the analysis indicates that the best fit is a simple linear one.

4. Results

4.1. Gridpoint univariate local regressions

We begin with a local regression of individual gridpoint SST time series *versus* the DRB streamflow time series. Figure 2a shows the resulting GCV score for each gridpoint univariate local regression, and indicates three SST regions with relatively low GCV scores, identified using black rectangles. Figure 2b shows the corresponding fraction of the 68-point dataset used for the localized subset regressions at each gridpoint, and indicates that the three low GCV score regions are also characterized by relatively small subsets. Hence, three coherent SST regions are identified which exhibit notable nonlinear relationships with subsequent DRB streamflow.

Based on general atmospheric circulation theory, these three SST regions can plausibly influence DRB streamflow. One region is in the Bering Sea (henceforth referred to as BS) underlying the Aleutian Low centre of the Pacific-North American (PNA) pattern, which is known to influence mid-latitude circulation over North America. The second region is located in the tropical Atlantic, off the coast of Africa (henceforth referred to as CA). SST anomalies in this region are known to initiate tropical cyclone activity that often reaches North America. The third region is located in the tropical Pacific, just west of Mexico (henceforth referred to as WM). This region underlies the subtropical jet which can carry moisture across southern North America, and is near the northern edge of the SST anomaly region associated with the El Nino-Southern Oscillation (ENSO) pattern. Hence, our analysis will focus on these three SST regions that are precursors of DRB streamflow.

4.2. Regional univariate local regressions

For each of the three regions identified in Figure 2, an area-weighted average SST time series is computed
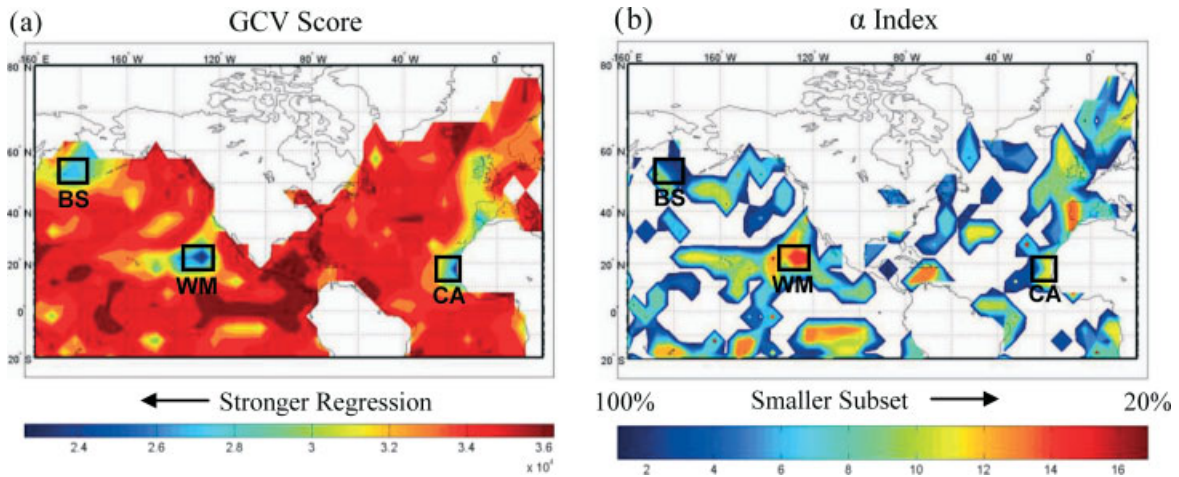
Figure 2. Univariate local regression results for AS gridpoint sea surface temperature *versus* ON DRB streamflow. (a) Generalized cross-covariance score, where smaller values indicate a stronger regression; (b) regression α index, where larger values indicate greater nonlinearity. Bering Sea (BS), Coast of Africa (CA) and West of Mexico (WM) regions delineated with black rectangles.
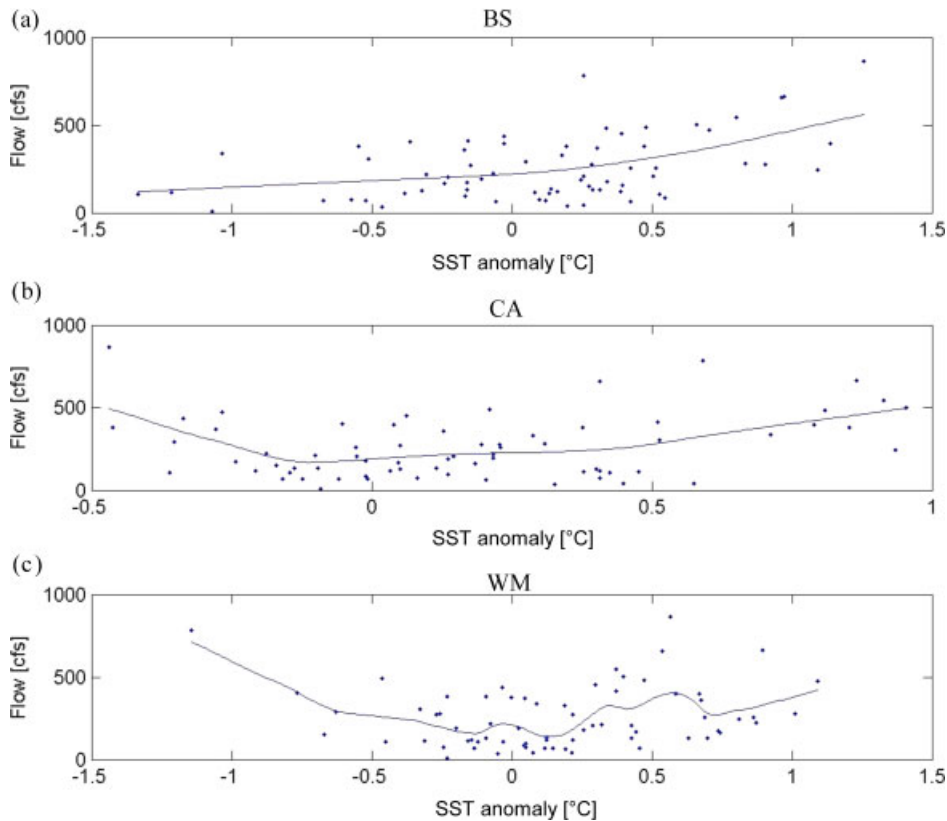

Figure 3. Univariate local regression results for AS regional sea surface temperature *versus* DRB ON streamflow. (a) Bering Sea; (b) Coast of Africa; and (c) West of Mexico. This figure is available in colour online at www.interscience.wiley.com/ijoc

and regressed against DRB streamflow. Results for each regional univariate local regression are presented in Figure 3. SST anomalies in the BS region exhibit a monotonically increasing relationship with subsequent DRB streamflow (Figure 3a). This is reasonable, as warmer SSTs generate more rising air and hence, lower atmospheric pressure over this region, which is characteristic of a positive PNA pattern and meridional circulation over North America. This can potentially carry more moisture northward from the Gulf of Mexico, along the eastern

seaboard of North America, and into the DRB region. Conversely, negative BS SSTs can lead to a negative PNA pattern, zonal circulation and hence, less moisture transport into the DRB region. However, Figure 3a indicates greater streamflow sensitivity to positive BS SST anomalies than negative ones, so that the overall relationship exhibits slight nonlinearity. Note that the PNA pattern is recognized to occur year round, although it tends to be weaker during the summer months (Climate Prediction Center, 2005).

Figure 3b shows the local regression result for the CA region. Elevated DRB streamflows appear to be related to large positive CA SST anomalies. This is expected, as warm SSTs in the tropical Atlantic initiate tropical cyclone activity that can evolve into tropical storms or hurricanes. These systems occasionally reach eastern North America, where their considerable precipitation results in elevated streamflow. However, a corresponding streamflow reduction does not materialize for negative CA SST anomalies. Figure 3b actually indicates elevated streamflows with greater negative SST anomalies, although there is no physical basis for this behaviour. It is likely influenced by one extreme data point (1977), with the coldest CA SST value but the highest DRB streamflow value. A review of tropical cyclone stormtracks for this year indicates that very little cyclone activity reached the eastern US (Jarvinen *et al.*, 1984) so that other processes are responsible for the elevated streamflows during this year. Note in Figure 3a that this year exhibits the highest BS SST value.

Figure 3c shows the local regression result for the WM region. As for the BS and CA regions, elevated DRB streamflows appear to be related to positive WM SST anomalies. This is also reasonable, as warmer SSTs in this region will allow for more evaporated moisture to be transported along the subtropical jet stream and into the eastern United States. Also, WM is near the northern fringe of the ENSO region, whose positive anomalies are generally associated with increased precipitation across much of the United States. As for the CA region, a corresponding streamflow reduction does not materialize for negative WM SST anomalies, and apparent elevated streamflows with greater negative SST anomalies are likely the result of one extreme data point (1955). Tropical cyclone activity reaching the eastern US was considerable for this year (Jarvinen *et al.*, 1984), which likely explains the elevated streamflows. This extreme data point is particularly influential as it is isolated from all other data points in Figure 3c and hence exerts considerable leverage on the regression.

The three univariate local regressions shown in Figure 3 have identified relationships between regional SST anomalies and DRB streamflow that are physically plausible, but nonlinear and asymmetric. Such complex behaviour would not have been detected using simple linear regression analyses. These nonlinearities exhibited by each regional regression partially mask the underlying physical relationship and are likely due to competing physical factors such as interactions between the various physical mechanisms. For example, the relatively low sensitivity to negative BS SST anomalies may be related to the WM region. Although a negative PNA pattern reduces moisture transport from the Gulf of Mexico, the zonal circulation across North America may facilitate moisture transport into eastern North America via the subtropical jet stream. Also, the streamflow response to CA SST is likely constrained to strong positive anomalies that produce tropical cyclones of sufficient frequency and magnitude, so that an appreciable number will track as

far as the DRB region. For all other years, other factors are likely to have a greater influence on DRB streamflow, so that a physically meaningful relationship with CA SST does not materialize.

4.3. Regional bivariate local regressions

In order to capture the apparent interaction between the different regional SST precursors for DRB streamflow, a series of bivariate local regressions are performed, as presented in Figure 4. The combined influence of the BS and CA regions (Figure 4a) shows elevated streamflows for positive BS SST anomalies (i.e. meridional circulation over NA), regardless of the state of CA SSTs. Streamflows are modestly reduced for negative BS SST anomalies, except for increased streamflows when CA SSTs are high, i.e. when tropical cyclone activity is likely. Conversely, negative CA SST anomalies have a negligible impact on streamflow. Figure 4a clearly shows nonlinear interactions between the BS and CA regions, and their combined effect on DRB streamflow is physically coherent.

The combined influence of the BS and WM regions (Figure 4b) similarly shows a dominant elevated streamflow response to positive BS SST anomalies, and a secondary elevated streamflow response to positive WM SST anomalies (i.e. a moist subtropical jet) when BS SSTs are average or low. Elevated streamflows are also associated with negative WM SST anomalies, although again this response may be unduly leveraged by the extreme 1955 data point in which frequent tropical cyclone activity resulted in elevated streamflows.

The combined influence of the CA and WM regions (Figure 4c) shows consistent elevated streamflows only for extreme positive CA SST anomalies, i.e. high tropical cyclone activity. Elevated streamflow in response to positive WM SST anomalies is less apparent compared to Figure 4b. Once again, the elevated streamflow response to negative WM SST anomalies is highly leveraged by the extreme 1955 data point, although positive CA SST anomalies during this year are consistent with the considerable tropical cyclone activity that occurred during this year. All three upper DRB water supply reservoirs exhibited similarly elevated inflow during this year (1955), hence tropical storm activity seems to be an influential factor. Nevertheless, nonlinear interactions involving WM SSTs appear to have a complicated combined effect on DRB streamflow.

This bivariate regression analysis reconciles the low CA SST, high streamflow 1977 data point in Figure 3b, as this data point (i.e. highest DRB streamflow over the 68-year period of record) also exhibits the highest BS SST as indicated in Figure 3a Hence, Figure 4a attributes this elevated streamflow value to the BS region rather than the CA region. Unfortunately, the low WM SST, high streamflow 1955 data point in Figure 3c is not as well reconciled. This data point (i.e. second highest DRB streamflow over the 68-year period of record) exhibits near-average BS SST values (Figure 3a) and elevated
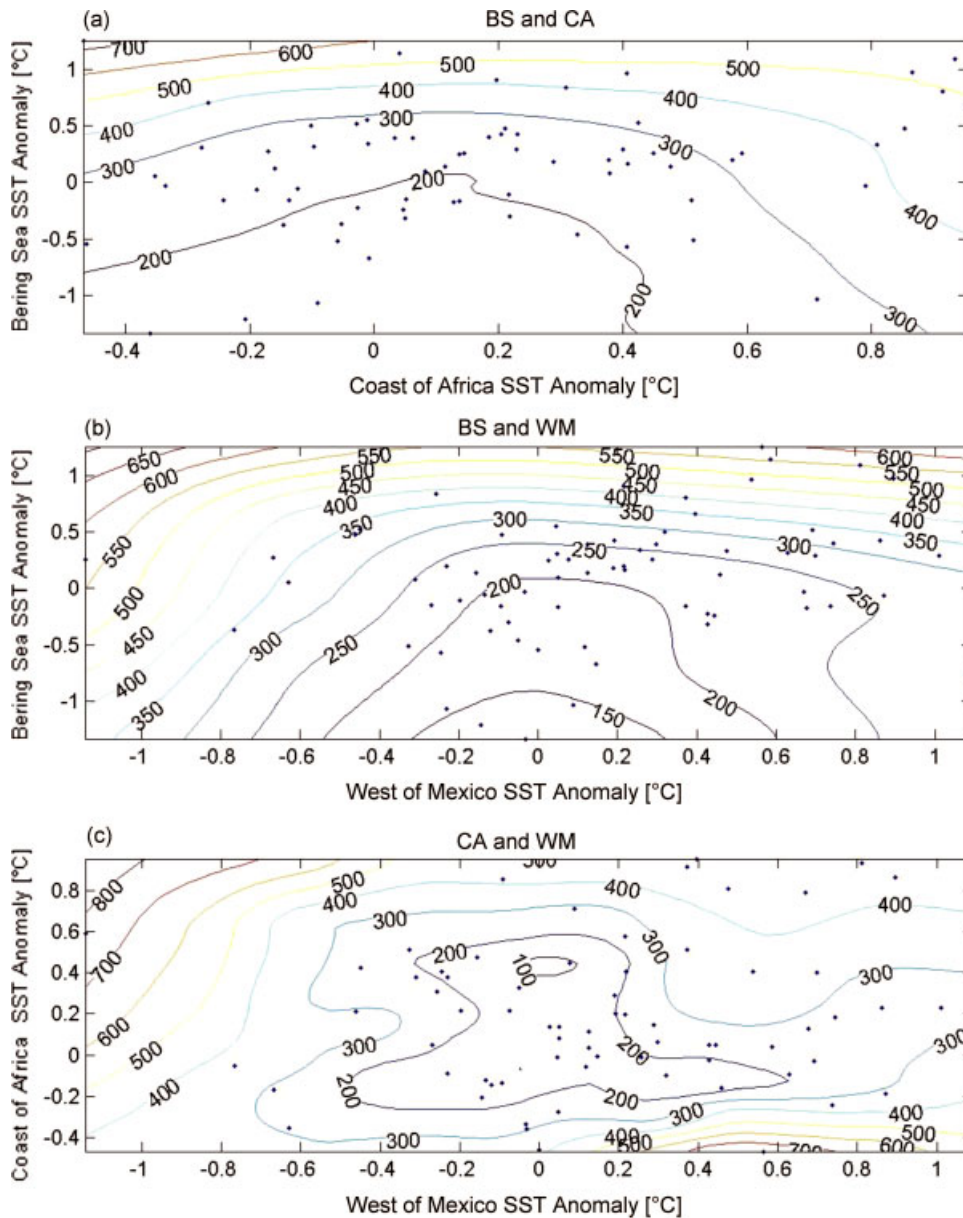
Figure 4. Bivariate local regression results for AS regional sea surface temperature *versus* DRB ON streamflow. Contours represent regressed streamflow values in cfs. (a) Bering Sea and Coast of Africa; (b) Bering Sea and West of Mexico; and (c) Coast of Africa and West of Mexico. This figure is available in colour online at www.interscience.wiley.com/ijoc

but not extreme CA SST values (Figure 3b). It is also far removed from other data points in Figure 3c. Hence, the bivariate regressions attribute the elevated streamflow during this year primarily to the WM region and yields a broad but highly leveraged elevated streamflow response to negative WM SST anomalies in Figure 4b and c.

4.4. Comparison of regression models

The results from the six regional local regression models (three univariate and three bivariate) are compiled in Table I. All models contain nonlinear relationships as indicated by subset fractions less than 1, with the univariate regression for the BS region being closest to linear. The bivariate models all yield stronger results than the univariate models, in terms of both lower GCV scores and larger fractions of the observed streamflow

Table I. Summary of regional local regression results.

SST predictors	Subset fraction	GCV	R^2
BS	0.90	26568	0.28
CA	0.50	26245	0.33
WM	0.25	27701	0.39
BS and CA	0.75	24182	0.45
BS and WM	0.75	24324	0.43
CA and WM	0.25	21097	0.68

variance captured (i.e. correlation R^2). This confirms that streamflow in the DRB region is not driven by a single dominant climatic phenomenon, but rather is influenced by a variety of climatic processes.

Among the bivariate models, the combination of WM and CA SSTs yields the strongest local regression relationship, explaining 0.68 of the upper DRB streamflow variability, which is statistically significant at the 99% level (i.e. $p < 0.01$). Figure 5 plots the time series of simulated DRB streamflows for this model against observations, and also the residual time series, histogram and probability plot. The local regression model replicates the basic features of the observed streamflow time series remarkably well, and the residuals are normally distributed. This result supports the notion that regional SSTs are nonlinear climatic precursors of autumn streamflow in the northeast US.

An analogous multiple linear regression is also performed to compare its performance against the local regression model. Gridpoint univariate linear regression results are shown in Figure 6, which reveal two regions that exhibit statistically significant (at the 95% level) linear correlation coefficients R between SST and DRB streamflow. These regions are displaced slightly from the previously defined BS and CA regions for the local regression, and so are referred to as BS′ and CA′, and delineated with black rectangles in Figure 6. Note that significant linear correlations are not found in the vicinity of the WM region chosen by local regression. The results of a bivariate linear regression model developed using SSTs averaged over the BS′ and CA′ regions are shown in Figure 7. This linear model performs notably worse than all six local regressions. Compared to the strongest local regression model, the GCV score is 36%

greater (28 588 *vs* 21 097), and the fraction of observed variance explained R^2 is 71% smaller (0.20 *vs* 0.68). The linear model time series exhibits considerably less interannual variability than observations, and the residuals are not normally distributed. For the region and season considered in this study at least, local regression appears to exhibit a marked improvement over linear regression, for detecting summer SST precursors of autumn streamflow.

4.5. Forecast potential

The local regression time series model shown in Figure 6 uses the full period of record to identify a historical relationship between autumn DRB streamflow and preceding summer regional SSTs. Specifically, the model simulated streamflow for a given year was regressed using a local subset of data that included the year being simulated. Seasonal forecasts of future DRB streamflows obviously cannot utilize streamflow data from the year being forecast. Therefore, to assess the forecast potential, leave-one-out cross-validation is applied to the local regression time series model, by excluding the year being simulated from the local regression subset for that year.

Figure 8 plots the resulting cross-validated local regression time series against observations. The strength of this model is considerably weaker than without cross-validation (Figure 5), e.g. the range of simulated streamflow values is substantially reduced. Also, only 0.13 of the observed streamflow variability is explained, which is less than for the full data local regression (0.68) and also
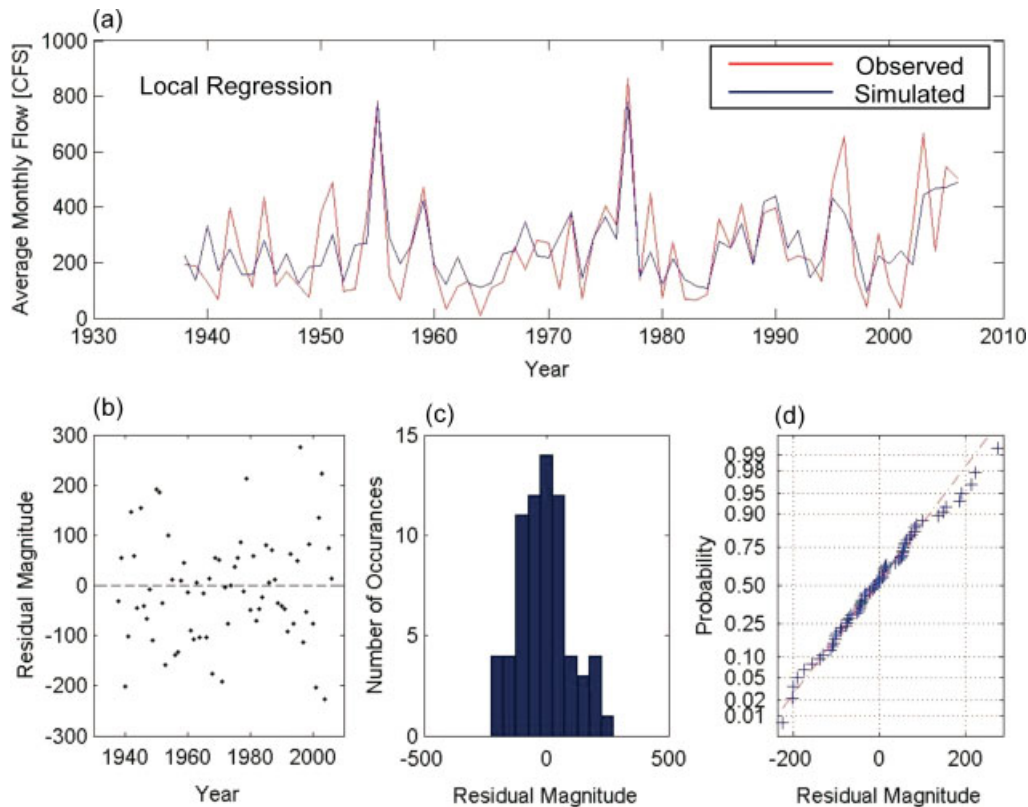

Figure 5. Bivariate local regression results for CA and WM region sea surface temperatures *versus* DRB ON streamflow. (a) Simulated *versus* observed time series; (b) residual time series; (c) residual histogram; and (d) residual normal probability plot.
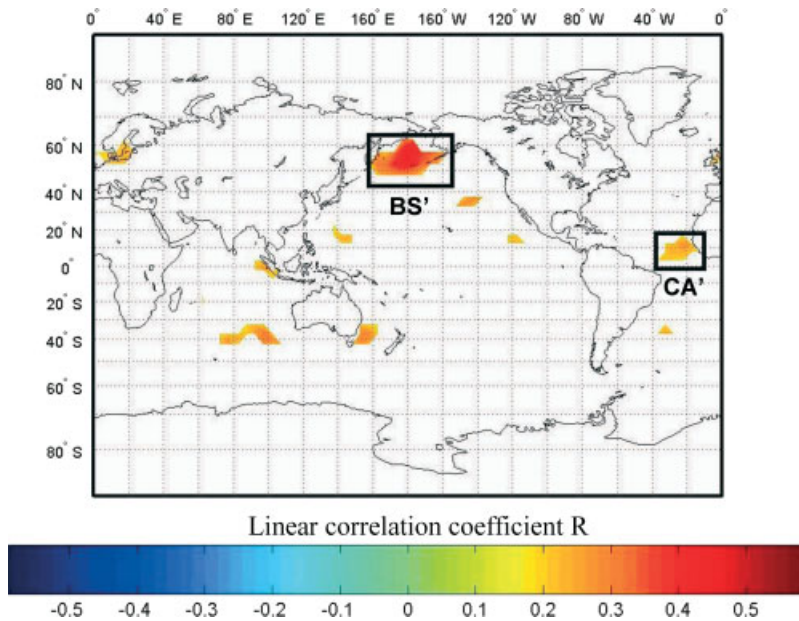
Figure 6. Univariate linear regression results for AS gridpoint sea surface temperature *versus* ON DRB streamflow. Only gridpoints with correlation coefficients R that are significant at the 95% level are shown. Bering Sea (BS′) and Coast of Africa (CA′) regions delineated with black rectangles.
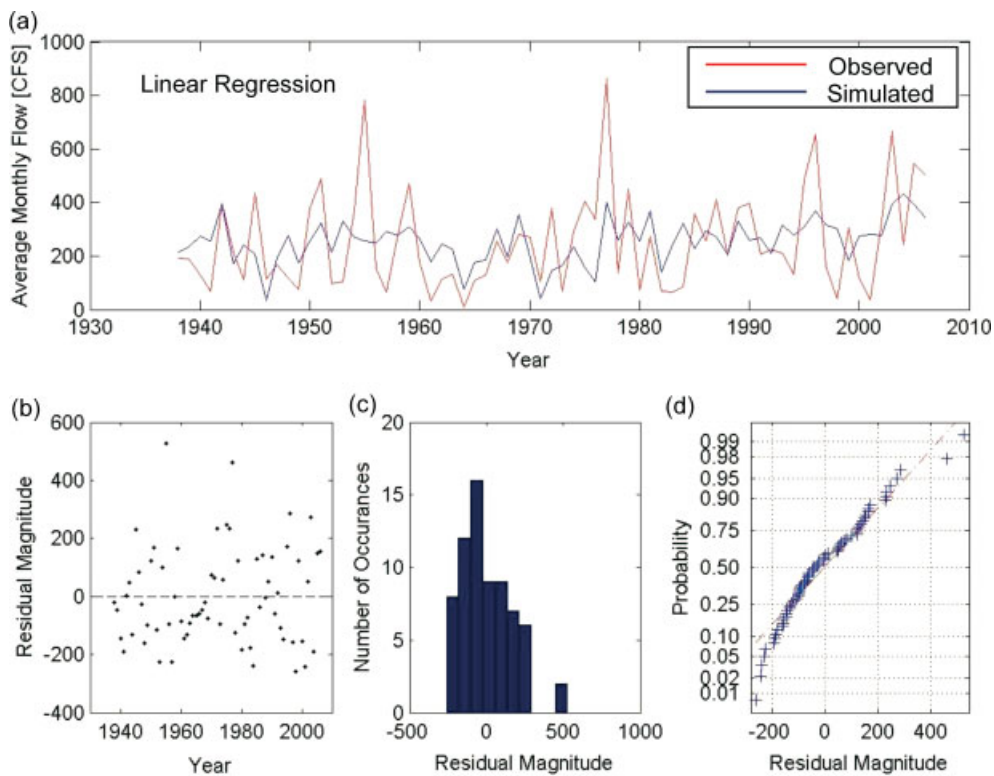

Figure 7. Bivariate linear regression results for BS and CA region sea surface temperatures *versus* DRB ON streamflow. (a) Simulated *versus* observed time series; (b) residual time series; (c) residual histogram; and (d) residual normal probability plot.

the linear regression (0.20). However, the cross-validated local regression does appear to capture low frequency variability better than the fitted (non-cross-validated) linear regression (Figure 7), e.g. the low streamflow periods during the early 1960s, the early 1980s and around the year 2000. Nevertheless, although the local regression identifies SST regions that are physically meaningful

precursors of DRB streamflow, these nonlinear relationships are not yet strong enough to produce useful forecasts.

Figure 8 also shows the 95% confidence limits for the cross-validated model. Observed streamflow for 6 years (indicated with black squares) fall outside of these confidence limits, which exceeds the 95% threshold
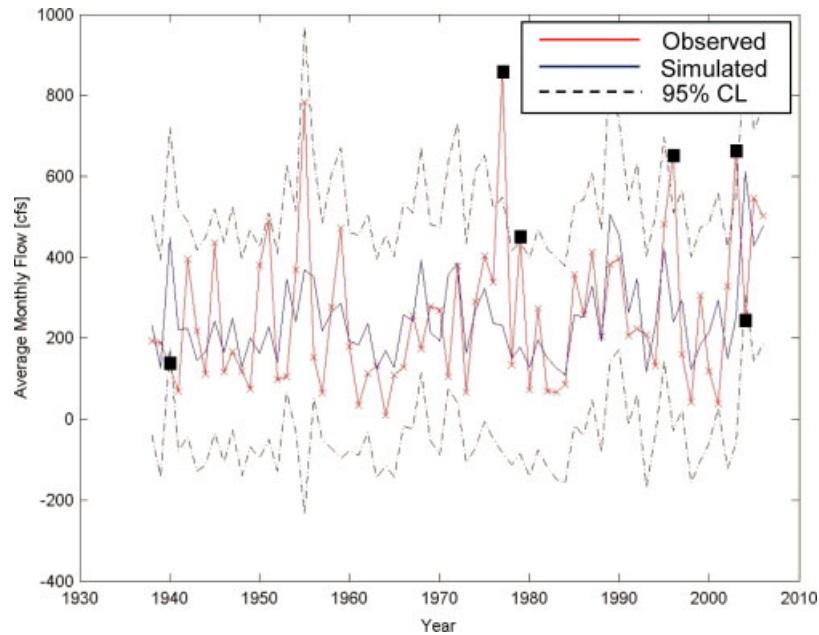
Figure 8. Cross-validated DRB ON streamflow forecast time series using bivariate local regression model for CA and WM region sea surface temperature predictors. Observations which fall outside of the 95% forecast confidence limits are denoted with black squares.

of 3.4 years expected for the 68-year dataset. Figure 9 shows where these 6 years reside in the state space of the two regression predictors. One data point resides near the average for both parameters, when anomalous streamflow values would likely be driven by factors other than the model predictors. This suggests that forecast skill may improve with the inclusion of other climatic predictors in addition to the BS and CA SST regions. The other five data points reside in areas of the state space that are somewhat removed from the rest of the data points, so that cross-validated regressions that exclude the data point would effectively eliminate the influence of that observation, and hence weaken the regression. This suggests that the forecast skill may improve with a longer period of record that increases the sampling frequency of these SST conditions.

5. Conclusions

This study identifies three regions whose summer SST values act as climatic precursors of autumn streamflow in the Delaware River Basin located in the northeast US. Each region has a physically plausible influence on DRB streamflow, arising from general circulation patterns and established cyclonic phenomena. Univariate local regression analyses detect nonlinearities in the streamflow response, and bivariate local regressions reveal some of the interactions that occur between these SST forcing regions. A bivariate local regression involving SSTs in regions west of Mexico and off the Atlantic coast of Africa yields the strongest statistical relationship, explaining 68% of the observed interannual streamflow variability. This represents a vast improvement over an analogous bivariate linear regression using the same two general SST regions, and a considerable improvement
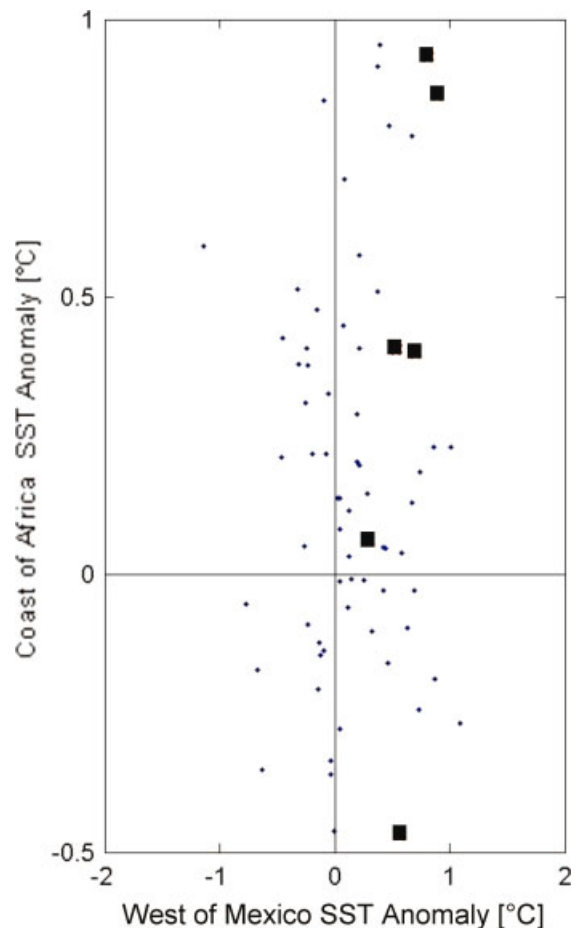

Figure 9. BS and CA region sea surface temperature predictor values over 68-year study period. Years in which observed streamflow falls outside of the 95% forecast confidence limits using these predictors are denoted with black squares. This figure is available in colour online at www.interscience.wiley.com/ijoc

over previous efforts to identify streamflow predictability in this region (Miller *et al.*, 2006). Although these gains are diminished under cross-validation, the nonlinear models, which typically reduce bias but have higher variance of estimation, still perform well relative to the non-cross-validated linear models.

These local regression analyses shed some light on the relationships that exist between DRB streamflow and preceding regional SSTs. Nonlinearities exist primarily in the form of asymmetries, i.e. the streamflow response to positive anomalies of a SST predictor is not equal and opposite to the response to negative anomalies. Such behaviour is not at all surprising given the complexities of the physical phenomena involved and their ability to influence one another. Moreover, the hydroclimatology of the DRB region is not dominated by any single one of these phenomena, so accounting for their interactions in a multivariate framework is crucial to improving the predictive potential of streamflow in this region. Analysis of intervening circulation variables could yield additional insights as to the precise mechanisms involved, although it would likely have little impact on predictive potential as the seasonal memory is contained in the SSTs.

Although the results of this study demonstrate stronger and more coherent streamflow precursors than have previously been identified in the literature, cross-validation indicates that translating these physically meaningful climate precursors into effective seasonal streamflow forecasts still poses a significant challenge. Additional research along these lines may be beneficial in this regard. A longer period of record could conceivably yield better results through improved coverage of the predictor state space region, thereby reducing the leverage of extreme data points, reducing estimation variance and improving both the simulation model and cross-validated forecasts. A multivariate local regression involving all three SST regions could also be performed. Nevertheless, this study has helped improve our understanding of climatic streamflow precursors in the northeast US and helped to establish its predictive potential. In future work, we expect to present a Bayesian non-parametric/nonlinear regression model where predictive uncertainty in nonlinear modelling is formally dealt with and multiple candidate models are optimally combined.

Finally, it is worth noting that seasonal average (total) flows are comprised of baseflow at the beginning of the season, baseflow recession subsequent to precipitation events and event runoff hydrographs. At the seasonal time scale, the first component may be determined by the SST-forced anomalous circulation and soil moisture during the preceding season, and hence potentially serve as another streamflow precursor. Meanwhile, the latter two components are effectively determined by the number of single and composite precipitation events and the cumulative event rainfall during the season being predicted. Often, the number of large precipitation events that contribute to a significant enhancement of seasonal precipitation and hence streamflow is small. Thus, it is useful to explore how source regions of moisture or steering of atmospheric circulation and water vapour transport correspond to the event frequency and amount characteristics. Although some promising preliminary work has been pursued in this direction, we expect to show an inter-comparison of GCM dynamics and re-analysis based reconstructions of the relevant statistics and their correspondence to the seasonal relationships to predictors in a future paper.

Acknowledgements

References

Barlow M, Nigam S, Berbery EH. 2000. ENSO, pacific decadal variability, and U.S. summertime precipitation, drought, and streamflow. *Journal of Climate* **14**: 2105–2128.

Bradbury JA, Dingman SL, Keim BD. 2002. New England drought and relations with large scale atmospheric circulation patterns. *Journal of the American Water Resources Association* **38**: 1287–1299.

Bradbury JA, Keim BD, Wake CP. 2003. The influence of regional storm tracking and teleconnections on winter precipitation in the northeastern United States. *Annals of the Association of American Geographers* **93**: 544–556.

Climate Prediction Center. 2005. The Pacific/North American Pattern. http://www.cpc.noaa.gov/data/teledoc/pna_map.shtml.

Dirmeyer PA, Fennessy MJ, Marx L. 2003. Low skill in dynamical prediction of boreal summer climate: grounds for looking beyond sea surface temperature. *Journal of Climate* **16**: 995–1002.

Fraser AM, Swinney HL. 1986. Independent coordinates for strange attractors from mutual information. *Phys. Rev. A* **33**: 1134–1140.

Gong G, Wang L, Condon L, Shearman A, Lall U. 2010. A simple framework for incorporating seasonal streamflow forecasts into existing water resource management practices. *Journal of the American Water Resources Association* (in press).

Gurka JJ, Auciello EP, Gigi AF, Waldstreicher JS, Keeter KK, Businger S, Lee LG. 1995. Winter weather forecasting throughout the eastern United States. Part II: an operational perspective of cyclogenesis. *Weather and Forecasting* **10**: 21–41.

Hartley S, Keables MJ. 1998. Synoptic associations of winter climate and snowfall variability in New England, USA. *International Journal of Climatology* **18**: 281–298.

Jarvinen BR, Neumann CJ, Davis MAS. 1984. A tropical cyclone data tape for the North Atlantic basin, 1886–1983: contents, limitations, and uses. *NOAA Technical Memorandum NWS NHC 22*, National Hurricane Center, Miami, FL. Updated May 5, 2009. http://weather.unisys.com/hurricane/atlantic/.

Joyce TM. 2002. One hundred plus years of wintertime climate variability in the eastern United States. *Journal of Climate* **15**: 1076–1086.

Jutla AS, Small D, Islam S. 2006. A precipitation dipole in eastern North America. *Geophysical Research Letters* **33**: L21703, DOI:10.1029/2006GL027500.

Kaplan A, Cane M, Kushnir Y, Clement A, Blumenthal M, Rajagopalan B. 1998. Analyses of global sea surface temperature 1856–1991. *Journal of Geophysical Research* **103**: 18567–18589.

Khan S, Ganguly AR, Bandyopadhyay S, Saigal S, Erickson DJ, Protopopescu V, Ostrouchov G III. 2006. Nonlinear statistics reveals stronger ties between ENSO and the tropical hydrological cycle. *Geophysical Research Letters* **33**: L24402, DOI:10.1029/2006GL027941.

Kingston DG, McGregor GR, Hannah DM, Lawler DM. 2006. River flow teleconnections across the northern North Atlantic region. *Geophysical Research Letters* **33**: L14705, DOI:10.1029/2006GL026574.

Lall U, Moon YI, Kwon HH, Bosworth K. 2006. Locally weighted polynomial regression: parameter choice and application to forecasts of the Great Salt Lake. *Water Resources Research* **42**: W05422, DOI:10.1029/2004WR003782.

Leathers DJ, Malin ML, Kluver DB, Henderson GR, Bogart TA. 2008. Hydroclimatic variability across the Susquehanna River Basin, USA, since the 17th century. *International Journal of Climatology* **28**: 1615–1626.

Loader C. 1999. *Local Regression and Likelihood*. Springer-Verlag: New York.

Marengo JA, Cavalcanti IFA, Satyamurty P, Trosnikov I, Nobre CA, Bonatti JP, Camargo H, Sampaio G, Sanches MB, Manzi AO, Castro CAC, D'Almeida C, Pezzi LP, Candido L. 2003. Assessment of regional seasonal rainfall predictability using the CPTEC/COLA atmospheric GCM. *Climate Dynamics* **21**: 459–475.

Miller WD, Kimmel DG, Harding LW Jr. 2006. Predicting spring discharge of the Susquehanna River from a winter synoptic climatology for the eastern United States. *Water Resources Research* **42**: W05414, DOI:10.1029/2005WR004270.

Moon YI, Lall U, Kwon HH. 2008. Nonparametric short term forecasts of the Great Salt Lake using atmospheric indices. *International Journal of Climatology* **28**: 361–370.

Moon YI, Rajagopalan B, Lall U. 1995. Estimation of mutual information using kernel density estimators. *Phys. Rev. E* **52**: 2318–2321.

Quan X, Hoerling M, Whitaker J, Bates G, Xu T. 2006. Diagnosing sources of U.S. seasonal forecast skill. *Journal of Climate* **19**: 3279–3293.

Sharma A. 2000a. Seasonal to interannual rainfall probabilistic forecasts for improved water supply management: Part 1 – a strategy for system predictor identification. *Journal of Hydrology* **239**: 232–239.

Sharma A. 2000b. Seasonal to interannual rainfall probabilistic forecasts for improved water supply management: Part 3 – a nonparametric probabilistic forecast model. *Journal of Hydrology* **239**: 249–258.

Sharma A, Luk KC, Cordery I, Lall U. 2000. Seasonal to interannual rainfall probabilistic forecasts for improved water supply management: Part 2 – predictor identification of quarterly rainfall using ocean-atmosphere information. *Journal of Hydrology* **239**: 240–248.

Sveinsson OGB, Lall U, Fortin V, Perrault L, Gaudet J, Zebiak S, Kushnir Y. 2008a. Forecasting spring reservoir inflows in Churchill Falls Basin in Quebec, Canada. *Journal of Hydrologic Engineering* **13**: 426–437.

Sveinsson OGB, Lall U, Gaudet J, Kushnir Y, Zebiak S, Fortin V. 2008b. Analysis of climatic states and atmospheric circulation patterns that influence Quebec spring streamflows. *Journal of Hydrologic Engineering* **13**: 411–425.

Vermette S. 2007. Storms of tropical origin: a climatology for New York State, USA (1851–2005). *Natural Hazards* **42**: 91–103.

Zishka KM, Smith PJ. 1980. The climatology of cyclones and anticyclones over North America and surrounding ocean environs for January and July, 1950–77. *Monthly Weather Review* **108**: 387–401.